Journal of Fluorine Chemistry 134 (2012) 29–34

Contents lists available at ScienceDirect

Journal of Fluorine Chemistry

journal homepage: www.elsevier.com/locate/fluor

Mixed metal^{II}–metal^{IV} hybrid fluorides

Jérôme Lhoste, Karim Adil, Armel Le Bail, Marc Leblanc, Annie Hémon-Ribaud, Vincent Maisonneuve *

Laboratoire des Oxydes et Fluorures, UMR CNRS 6010, Faculté des Sciences et Techniques, Université du Maine, Avenue Olivier Messiaen, 72085 Le Mans Cedex 09, France

ARTICLE INFO

Article history:
Received 26 January 2011
Received in revised form 25 March 2011
Accepted 28 March 2011
Available online 5 April 2011

Keywords:
Hybrid fluorides
Hydrothermal synthesis
Microwave heating

ABSTRACT

Six M^{II}–M^{IV} type II hybrid fluorides (M^{II} = Cu, Ni; M^{IV} = Si, Ti, Mo) are compared: $(Ni(en)_3)\cdot(TiF_6)$, $[Hpy]_2\cdot(Cu(py)_4(MF_6)_2)$ (M^{IV} = Ti, Mo), $[H_3O]_2\cdot(SiF_6(CuF(py)_4)_2)\cdot(F)_2$ and $Cu(en)_2MF_6$ (M^{IV} = Ti, Si). They are obtained at 160 °C under microwave heating and the structures are determined either from single crystal or powder X-ray diffraction data. All phases involve neutral amines that are linked to M^{II} cations, a feature of type II hybrids. In $(Ni(en)_3)\cdot(TiF_6)$, the cationic $(Ni(en)_3)^{2+}$ and anionic $(TiF_6)^{2-}$ entities are isolated. In $[Hpy]_2\cdot(Cu(py)_4(TiF_6)_2)$ and $[Hpy]_2\cdot(Cu(py)_4(MoF_6)_2)$, extra non metal bonded amines are protonated to give $[Hpy]^+$ cations that exchange hydrogen bonds with fluoride anions, a feature of type I hybrids. All phases exhibit a fully fluorinated octahedral environment of M^{IV} cations, at the opposite from previously reported $[H_3O]_2\cdot(NbOF_5(CuF(py)_4)_2)\cdot(F)_2$ or $[Hpy]_2\cdot(Cu(py)_4)(MoO_2F_4)_2$. In $[Hpy]_2\cdot(Cu(py)_4(MF_6)_2)$ (M^{IV} = Ti, Mo) or $[H_3O]_2\cdot(SiF_6(CuF(py)_4)_2)\cdot(F)_2$, Cu^{II} and M^{IV} entities are associated by fluoride anions to give anionic or neutral trimetallic clusters, respectively; the results of thermal analysis suggest that the oxidation state is +IV for molybdenum and it is proposed that H_3O^+ and "free" F^- ion pairs can be replaced locally by H_2O and HF couples. In $Cu(en)_2MF_6$, the Cu^{II} and M^{IV} entities alternate and build infinite chains

1. Research topics

The *Laboratoire des Fluorures* was created in 1965 by Prof. R. De Pape and was specialized in the synthesis and the structural and magnetic investigations of inorganic fluorides and oxyfluorides. Research on fluoride glasses started in 1980. At the end of the nineties, both oxides and fluorides were investigated and the laboratory was then entitled *Laboratoire des Oxydes et Fluorures* (LdOF). Today, 10 researchers work on Fluorides. The activity is mainly concerned with the elaboration and the characterization of crystallized and glassy fluorides as well as structural investigation by solid state NMR and NMR parameter calculations.

Hydrothermal growth of crystallized materials has been devoted to transition metal fluorides and, later, to fluoride carbonates. Recently, the research projects on crystalline fluorides have shifted towards hybrid fluorometallates and nanosized inorganic fluorides. These materials are prepared under solvothermal conditions, eventually assisted by microwave heating. The structures are determined from single-crystals or powders and the thermal behaviors are explored. The design of experiments approach is applied to optimize the material properties. The main goal is to demonstrate that crystalline fluoride materials could be a valid alternative in energy area such as gas storage, catalysis or batteries.

First dedicated to the quest of new compositions and related structural studies, the activities on fluoride glasses are now focused on the fabrication of rare-earth doped glassy waveguides, obtained by physical vapor deposition using co-evaporation. An expertise in rare earth ions interactions and upconversion phenomena has also been developed. More recently, glass ceramics, which combine the advantages of optical glass with crystal-like spectroscopic characteristics of rare-earth ions, have been prepared. These materials open potentialities for the miniaturization of optical devices, such as optical amplifiers and laser microsources.

In collaboration with the *Laboratoire de Physique de l'Etat Condensé*, the activities and projects related to solid state NMR concern the structural characterizations of more or less disordered fluorinated materials (oxyfluorides, nanostructured hydroxyfluorides, etc.), first-principle computations of NMR parameters (isotropic chemical shift, quadrupolar parameters and J-coupling) and structure determinations by coupling multinuclear and/or multidimensional solid state NMR, powder diffraction and *ab initio* calculations.

2. Introduction

The hydro(solvo)thermal synthesis of crystalline inorganic–organic hybrid materials implies polymerization reactions and

* Corresponding author. Tel.: +33 2 4383 3561; fax: +33 2 4383 3506.
E-mail address: vincent.maisonneuve@univ-lemans.fr (V. Maisonneuve).

0022-1139/$ – see front matter © 2011 Elsevier B.V. All rights reserved.
doi:10.1016/j.jfluchem.2011.03.021

Table 1
Class II mixed metal hybrid fluorides.

Entity	Dimensionality	Cheetham notation [24]	CSD code	Ref.
Cu(*py*)$_4$(ZrF$_6$)$_2$	cluster	I^0O^0	NAQJUK	[8]
Cu(*dmpyz*)$_4$SiF$_6$	*trans* chain	I^1O^0	LIQLED	[25]
Zn(*4-4′pdbpy*)$_2$SiF$_6$	*trans* chain	I^1O^0	BUPGEZ	[26]
Cu(*phpz*)$_4$SiF$_6$	*trans* chain	I^1O^0	JAJKIO	[27]
Co(*viz*)$_4$SiF$_6$	*trans* chain	I^1O^0	BOHFAF	[28]
Cu(*2-4′bpy*)$_4$SiF$_6$	*cis–trans* chain	I^1O^0	RERVIU	[17]
Cu(*4-phpy*)$_4$SiF$_6$	*cis–trans* chain	I^1O^0	RERVOA	[17]
Cu(*pyz*)$_2$SbF$_6$	chain	I^0O^1	SUPSUS	[29]
Cu(*pyz*)(H$_2$O)$_2$SiF$_6$	layer	I^1O^1	FUDQAX	[16]
Cu(*pyz*)(H$_2$O)$_2$TiF$_6$	layer	I^1O^1	WAFQEA	[15]
Cu(*pyz*)$_3$SiF$_6$	layer	I^1O^1	FUDQEB	[16]
Zn(*4-4′pbpy*)$_2$SiF$_6$	layer	I^1O^1	GELJEN	[30]
Zn(*4-4′edbpy*)$_2$SiF$_6$	layer	I^1O^1	HUKSEM	[31]
Zn(*4-4′edbpy*)$_2$SiF$_6$	layer	I^1O^1	HUKSIQ	[31]
Zn(*4-4′bdbpy*)$_2$SiF$_6$	layer	I^1O^1	HUKSOW	[31]
Zn(*S-S′ecbpy*)$_2$SiF$_6$	layer	I^1O^1	HUKSUC	[31]
Cu(*4,4′-bpy*)$_2$GeF$_6$	3D	I^1O^2	AFEHUO	[32]
Cu(*4,4′-bpy*)$_2$SiF$_6$	3D	I^1O^2	GORWUF AFEKAX	[32,33]
Zn(*4,4′-bpy*)$_2$SiF$_6$	3D	I^1O^2	ZESFUY WONZIJ	[34,35]
Zn(*pyz*)$_2$SiF$_6$	3D	I^1O^2	FUDQIF	[16]
Cu(*py*)$_4$TiF$_6$	3D	I^1O^2	JOLQAC	[36]
Zn(*4-4′dsbpy*)$_2$SiF$_6$	3D	I^1O^2	LEMMAS	[37]
Cu(*3-mepy*)$_4$VF$_6$	3D	I^1O^2	ROHCIB	[38]
Zn(*1-2eybpy*)$_2$SiF$_6$	3D	I^1O^2	WONZOP	[35]
Zn(*1-4bzbpy*)$_2$SiF$_6$	3D	I^1O^2	WONZUV	[35]

py = pyridine; *dmpyz* = 2,6-dimethylpyrazine; *4-4′pdbpy* = 4,4′-(pentane-1,5-diyldisulfanediyl) bipyridine; *phpz* = 5-phenyl-pyrazole; *viz* = N-vinyl-imidazole; *2-4′bpy* = 2,4′-bipyridine; *4-phpy* = 4-phenylpyridine; *pyz* = pyrazine; *4-4′pbpy* = 4,4′-(propane-1,5)bipyridine; *4-4′edbpy* = 4,4′-(ethane-1,2-diyldisulfanediyl)bipyridine; *4-4′bdbpy* = 4,4′-(butane-1,4-diyldisulfanediyl)bipyridine *S-S′ecbpy* = S,S′-(ethane-1,2-diylbipyridine-4-carbothioato); *4,4′-bpy* = 4,4′-bipyridine; *4-4′dsbpy* = 4,4′-bipyridyldisulfide; *3-mepy* = 3-methylpyridine; *1-2eybpy* = 1,2-bis(4-pyridyl)ethyne; *1-4bzbpy* = 1,4-bis(4-pyridyl)benzene.

leads to two types of hybrid networks [1] according to the synthesis conditions (pH, temperature, nature of structure directing agents, solvent, etc.). With oxyanion-based inorganic components, the search of new hybrid materials is very successful and consequently frenetic while the phases with purely fluorinated metal cations are scarce. Class I hybrids with weak interactions (Van der Waals or hydrogen bonds) between the organic and inorganic parts are well represented in such fluorides. All inorganic dimensionalities are encountered but only four compounds exhibit a tridimensional inorganic network; a comprehensive recent review is given in [2]. Few fluorides belong to class II hybrids in which metal atoms are strongly linked to the organic moieties by covalent or iono-covalent bonds. Most of the evidenced compounds are based on divalent (Cu, Zn) and tetravalent (Si, Ti, Ge) metals and pyridine or pyrazine amines and derivatives. The structures reveal cluster (0D), chains (1D), layered (2D) or framework structures (3D) (Table 1). Currently, we focus our work on new microporous type II fluorides by adding metal cations prone to accept nitrogen atoms in their coordination spheres. Pyridine (*py*) and, eventually ethylene diamine (*en*), are added in order to provide such nitrogen atoms. This paper reports on the solvothermal synthesis assisted by microwave heating of six type II mixed metal hybrid fluorides with 0D and 1D dimensionalities; they are based on M^{II} and M^{IV} elements and on pyridine or ethylene diamine.

Table 2
Proportions of the starting materials (molar ratio) for the synthesis of mixed metal(II)–metal(IV) hybrid fluorides.

$M^{IV}O_2/M^{II}O$/HF/*py*/*en*/EtOH	Compound	Cheetham notation [24]	Entity
1/1/11/49/4/136	(Ni(*en*)$_3$)·(TiF$_6$) (**1**)	I^0O^0	monomer
1/1/27/23/0/172	(H*py*)$_2$·(Cu(*py*)$_4$(TiF$_6$)$_2$) (**2**)	I^0O^0	trimer
1/1/27/23/0/172	(H*py*)$_2$·(Cu(*py*)$_4$(MoF$_6$)$_2$) (**3**)	I^0O^0	trimer
1/1/27/23/0/172	[H$_3$O]$_2$·(SiF$_6$(CuF(*py*)$_4$)$_2$)·(F)$_2$ (**4**)	I^0O^0	trimer
1/1/11/49/2/136	Cu(*en*)$_2$TiF$_6$ (**5**)	I^1O^0	chain
1/1/11/49/2/136	Cu(*en*)$_2$SiF$_6$ (**6**)	I^1O^0	chain

3. Results and discussion

Six new M^{II}–M^{IV} hybrid fluorides (M^{II} = Cu, Ni; M^{IV} = Si, Ti, Mo) are obtained by solvothermal synthesis at 160 °C under microwave heating. The proportions of the starting materials are indicated in Table 2. Crystals appear for three phases and microcrystalline powders for the other three phases; crystallographic data and intensity collection parameters are given in Table 3.

Table 3
Crystallographic data of (Ni(*en*)$_3$)·(TiF$_6$) (**1**), [H*py*]$_2$·(Cu(*py*)$_4$(TiF$_6$)$_2$) (**2**), [H*py*]$_2$·(Cu(*py*)$_4$(MoF$_6$)$_2$) (**3**), [H$_3$O]$_2$·(SiF$_6$(CuF(*py*)$_4$)$_2$)·(F)$_2$ (**4**), Cu(*en*)$_2$TiF$_6$ (**5**), and Cu(*en*)$_2$SiF$_6$ (**6**) at room temperature.

Compound	**1**	**2**	**3**	**4**	**5**	**6**
Formula weight (g mol^{-1})	400.87	863.91	927.79	1016.04	345.50	325.85
Crystal system	Hexagonal	Tetragonal	Tetragonal	Tetragonal	Orthorhombic	Orthorhombic
Space group	$P6_322$	$I4/mmm$	$I4/mmm$	$I4_1/acd$	$Cmca$	$Cmca$
a (Å)	9.200(1)	10.881(2)	10.970(1)	24.937(3)	14.455(1)	14.314(6)
b (Å)					10.084(1)	7.800(3)
c (Å)	9.762(1)	16.649(4)	16.704(1)	14.728(2)	7.878(1)	9.930(3)
V (Å^3), Z	715.6(1), 2	1971.2(5), 2	2010.4(1), 2	9159(4), 8	1148.2(1), 4	1108.7(7), 4
Wavelength (Å)	1.54056	0.71069	1.54056	0.71069	1.54056	0.71069
μ (mm^{-1})		1.01		1.11		2.14
$\rho_{calc.}$ (g cm^{-3})	1.860	1.456	1.533	1.474	1.999	1.952
2θ range (°)	5–100	3–60	5–90	3–64	7–90	3–60
Refl. meas.		1274		126728		941
Refl. uni.	400	807	635	3973	549	810
Refl. ($I > 2\sigma(I)$)		602		2126		435
Refined parameters	41	59	27	165	33	43
R/R_w		0.051/0.141		0.037/0.109		0.0417/0.118
R_p/R_{wp}	0.114/0.085		0.144/0.146		0.153/0.111	
R_B/R_f	0.031/0.064		0.084/0.075		0.059/0.204	
Goodness of fit		1.332		1.004		1.006
$\Delta\rho_{min}/\Delta\rho_{max}$ (eÅ^{-3})		−0.37/0.32		−0.47/0.41		−0.63/0.57

Crystallographic data for the structures have been deposited with the Cambridge Crystallographic Data Center, CCDC Nos. 809584 (**1**), 809590 (**2**), 809591 (**3**), 809592 (**4**), 809593 (**5**) and 809594 (**6**). Copies of data can be obtained, free of charge, on application to the Director, CCDC, 12 Union Road, Cambridge CB2 1EZ, UK (fax: +44 1223 336033 or e-mail: deposit@ccdc.cam.ac.uk).

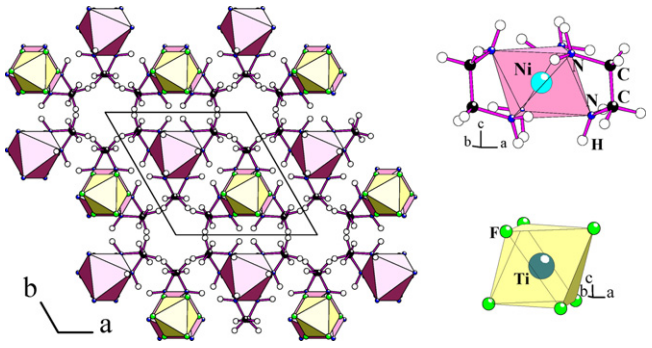

Fig. 1. [0 0 0 1] projection of the structure of $(Ni(en)_3)\cdot(TiF_6)$ (**1**) (left) and view of the isolated $Ni(en)_3$ and TiF_6 entities.

All M^{II} and M^{IV} cations adopt an octahedral coordination, strongly distorted for Cu^{2+} or Ni^{2+}. The M^{II}–N, M^{II}–F and M^{IV}–F distances are fairly consistent with the sum of atomic radii.

3.1. Isolated octahedra in $(Ni(en)_3)\cdot(TiF_6)$ (1)

The structure of $(Ni(en)_3)\cdot(TiF_6)$ (**1**) is built up from isolated $(TiF_6)^{2-}$ anions weakly hydrogen bonded to $(Ni(en)_3)^{2+}$ cations (Fig. 1). Ni^{2+} and Ti^{4+} cations lie on 2c and 2d sites of $P6_322$ space group and all Ni–N (2.101(5) Å) or Ti–F (1.823(4) Å) distances are equal. Ni^{2+} is coordinated by six nitrogen atoms coming from three neutral amines. The NiN_6 octahedron is strongly distorted: the N–Ni–N angle associated to nitrogen atoms of one discrete ethylene diamine molecule is 79.4(3)°. The TiF_6 octahedra are more regular and every fluoride anion is surrounded by three amines with N–H···F distances ranging from 3.08 Å to 3.22 Å. The packing of the $(Ni(en)_3)^{2+}$ cations leaves infinite channels and cavities along the 6_3 screw axis.

Three $M^{II}M^{IV}$ fluorides and one $M^{III}M'^{III}$ fluoride are isostructural with $(Ni(en)_3)\cdot(TiF_6)$ [3–6]. The evolution of the M–N and M–F distances is in agreement with the variations of the ionic radii of M^{II}, M^{III} or M^{IV} cations (Table 4). Ethylenediamine molecules adopt a *cis* conformation with a dihedral angle N(1)–C(1)–C(1)–N(1) ranging from 49.9 to 54.0°.

Table 4
Selected inter-atomic distances (Å) and angles (°) in $(M^{II}(en)_3)\cdot(M^{IV}F_6)$ and $(Co^{III}(en)_3)\cdot(Ga^{III}F_6)$ compounds.

ZnSi	Ni–Si	NiTi	NiGe	CoGe	$Co^{III}Ga^{III}$
Zn–N	Ni–N	Ni–N	Ni–N	Co–N	Co^{III}–N
2.186	2.123	2.101(5)	2.132	2.171	1.969
Si–F	Si–F	Ti–F	Ge–F	Ge–F	Ga^{III}–F
1.694	1.681	1.823(4)	1.793	1.794	1.891
N–Zn–N	N–Ni–N	N–Ni–N	N–Ni–N	N–Co–N	N–Co–N
80.2	81.6	79.4(3)	81.6	80.4	86.0

3.2. Clusters

3.2.1. Anionic clusters $(Cu^{II}(py)_4(M^{IV}F_6)_2)^{2-}$

In the structure of $[Hpy]_2\cdot(Cu(py)_4(MF_6)_2)$ (M^{IV} = Ti (**2**), Mo (**3**)), Cu^{II} atoms are octahedrally coordinated by four nitrogen atoms of four neutral pyridine molecules and by two fluorine atoms of two $M^{IV}F_6$ octahedra (Table 5). Anionic $(Cu(py)_4(MF_6)_2)^{2-}$ trimers result; seven atoms (F(3)–M–F(1)–Cu–F(1)–M–F(3)) are aligned and oriented along the *c* axis while copper bonded pyridine molecules lie in the (1 1 0) or (1 $\bar{1}$ 0) planes (Fig. 2). Disordered $[Hpy]^+$ cations ensure the electroneutrality of the structure; they lie at $z = 0.25$ together with equatorial F(2) fluorine atoms of the MF_6 octahedra with which they exchange N(2)–H···F(2) hydrogen bonds.

Taking into account the very close values of the diffusion factors for oxide and fluoride anions, three anion formulations are acceptable for $[Hpyr]_2\cdot(Cu(pyr)_4(MoF_6)_2)$: $(Mo^{IV}F_6)^{2-}$, $(Mo^{V}OF_5)^{2-}$ and $(Mo^{VI}O_2F_4)^{2-}$. The accuracy on bond distances that results from the structure determination with powder diffraction data is not sufficient to assess properly the oxidation state of molybdenum from bond valence calculations. A thermogravimetric experiment was then performed and MoO_2 resulted from the decomposition and the hydrolysis of the fluoride above 500 °C. The experimental and theoretical weight losses, 71.1% and 73.3%, respectively, are in good agreement with this observation, consistent with the presence of Mo^{IV} in $[Hpyr]_2\cdot(Cu(pyr)_4(MoF_6)_2)$. It must be noted that $[Hpy]_2\cdot(Cu(py)_4(TiF_6)_2)$ decomposes under heating to give $2TiO_2$

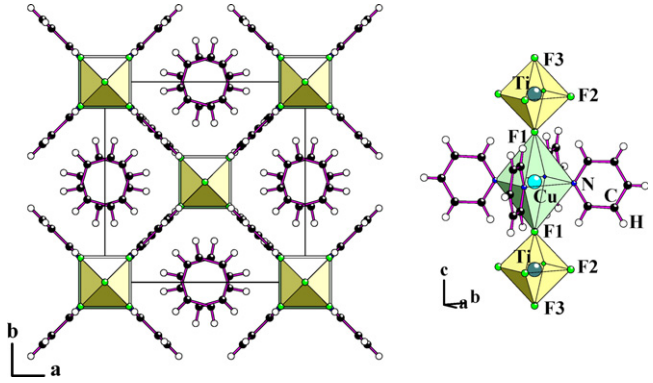

Fig. 2. [0 0 1] projection of the structure of $[Hpy]_2\cdot(Cu(py)_4(TiF_6)_2)$ (**2**) (left) and view of the $Cu(py)_4(TiF_6)_2$ cluster (right).

Table 5
M–X (X = N, O, F) distances (Å) in the anionic $M^{II}(py)_4(MX_6)_2$ trimers of $[Hpy]_2\cdot(Cu(py)_4(TiF_6)_2)$ (**2**), $[Hpy]_2\cdot(Cu(py)_4(Mo^{IV}F_6)_2)$ (**3**), $[Hpy]_2\cdot(Cu(py)_4(ZrF_6)_2)$, $[Hpy]_2\cdot(Cu(py)_4(Nb^{V}OF_5)_2)$, $[Hpy]_2\cdot(Cu(py)_4(V^{V}OF_5)_2)$, $[Hpy]_2\cdot(Cu(py)_4(Mo^{VI}O_2F_4)_2)$, $[Hpy]_2\cdot(Cu(py)_4(W^{VI}O_2F_4)_2)$ and $[Hpy]_2\cdot(Cd(py)_4(Nb^{V}OF_5)_2)$.

	$CuTi_2$ (**2**)	$CuMo_2$ (**3**)	$CuZr_2$	$CuNb_2$	CuV_2	$CuMo_2$	CuW_2	$CdNb_2$
X	Cu–X	Cu–X	Cu–X	Cu–X	Cu–X	Cu–X	Cu–X	Cd-X
O				2.406 × 2			2.407 × 2	2.333 × 2
N	2.025(4) × 4	2.13(1) × 4	2.042 × 4	2.052 × 2	2.035 × 2	2.035 × 2	2.038 × 2	2.333 × 2
				2.064 × 2	2.036 × 2	2.041 × 2	2.043 × 2	2.359 × 2
F(1)	2.507(4) × 2	2.49(2) × 2	2.452 × 2		2.459 × 2	2.437 × 2		

Ti^{IV}–F		Mo^{IV}–F		Zr^{IV}–F		Nb^{V}–X		V^{V}–X		Mo^{VI}–X		W^{VI}–X		Nb^{V}–X	
F(3)	1.813(5)	F(3)	1.73(2)	F3	1.963	O1	1.740	O1	1.595	O2	1.697	O1	1.760	O1	1.750
						F2	1.929	F4	1.811	O1	1.709	OF	1.884	F1	1.932
F(2)	1.857(2) × 4	F(2)	1.774(5) × 4	F2	1.999 × 4	F2	1.929	F2	1.819	F4	1.918	OF	1.885	F1	1.933
						F1	1.933	F5	1.836	F3	1.939	OF	1.899	F2	1.936
F(1)	1.899(4)	F(1)	2.04(2)	F1	2.048	F1	1.933	F3	1.882	F1	2.058	OF	1.903	F2	1.936
						F3	2.098	F1	2.084	F2	2.114	F3	2.021	F3	2.095

Table 6
M–X (X = N, O, F) distances (Å) in the neutral $MX_6(CuF(py)_4)_2$ trimers of isostructural $[H_3O]_2{\cdot}(SiF_6(CuF(py)_4)_2){\cdot}(F)_2$ (**4**), and $[H_3O]_2{\cdot}(NbOF_5(CuF(py)_4)_2){\cdot}(F)_2$.

	Cu_2Si (**4**)	Cu_2Nb	
X	Cu–X	Cu–X	
N	2.064(2) × 2	2.039 × 2	
	2.066(2) × 2	2.056 × 2	
F(1)	2.489(1)	(O,F)	2.291
	2.517(2)	F(4)	2.678
Si^{IV}-F		Nb^{V}-(O,F)	
F(2)	1.698(2) × 2	(O,F)	1.903 × 2
F(3)	1.701(2) × 2	F(2)	1.930 × 2
F(1)	1.741(2) × 2	F(3)	1.934 × 2

and 1/2Cu_2O; the experimental weight loss is 73.2% (Th. 73.2%). Thermal analyses are given as Supplementary Information.

3.2.2. Neutral cluster $M^{IV}F_6(Cu^{II}F(py)_4)_2$

In the structure of $[H_3O]_2{\cdot}(SiF_6(CuF(py)_4)_2){\cdot}(F)_2$ (**4**), the coordination of M^{II} and M^{IV} metals is identical with that found in the previous $(Cu(py)_4(MF_6)_2)^{2-}$ clusters (see Section 3.2.1). However, in **4**, the $Si^{IV}F_6$ octahedron is now central and the $SiF_6(CuF(py)_4)_2$ cluster is neutral (Table 6). Seven atoms (F(4)–Si–F(1)–Cu–F(1)–Si–F(3)) are also aligned and the clusters are oriented along two perpendicular directions, [1 1 0] or [1 $\bar{1}$ 0], while the planes of pyridine molecules lie in three perpendicular planes, (1 1 0), (1 $\bar{1}$ 0) or (0 0 1) (Fig. 3). These clusters leave infinite [0 0 1] channels along $\bar{4}$ symmetry axes where free fluoride and oxygen atoms are localized; these atoms are statistically distributed over symmetry related positions with site occupancy factors $\tau = 0.5$. Several hydrogen positions were obtained from Fourier difference syntheses; they are compatible with the presence of H_3O^+ cations and F^- anions or H_2O and HF molecules. Then, it is possible to define different orientations and hydrogen bonding schemes for H_3O^+ cations, H_2O or HF molecules and free F^- anions; several possibilities are illustrated in Fig. 4. A short range order is assumed while the long range stacking along *c* explains the observed disorder. The existence of such HF, H_2O molecules or H_3O^+ cations must be confirmed by spectroscopy techniques. This difficulty to localize the hydrogen atoms was also encountered in isostructural $[H_3O]_2{\cdot}(NbOF_5(CuF(py)_4)_2){\cdot}(F)_2$ [7]. In this last phase, the positions of hydrogen atoms are approximate and H_3O^+ cations are almost planar; it must be noted that oxygen atoms of $NbOF_5$ octahedra are statistically distributed with fluorine atoms on the axial bonding positions between copper and niobium octahedra.

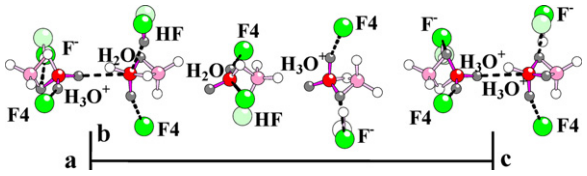

Fig. 4. Possible environments of H_3O^+ and F^- in $[H_3O]_2{\cdot}(SiF_6(CuF(py)_4)_2){\cdot}(F)_2$ (**4**) and eventual existence of H_2O and HF molecules. Non occupied positions of fluorine and oxygen atoms are given in light colours; occupied positions of hydrogen atoms are grey shaded.

3.2.3. Comparison of trimetallic clusters

Several anionic trimetallic clusters were previously reported in Cu^{II} or Cd^{II} fluorides or oxyfluorides. $[Hpy]_2{\cdot}(Cu(py)_4(Zr^{IV}F_6)_2)$ [8] is isostructural with the Ti^{IV} (**2**) and Mo^{IV} (**3**) phases that are described in Section 3.2.1 (Table 5) and five other similar phases with Cu/Nb^V [9,10], Cu/V^V [11], Cu/Mo^{VI} [8], Cu/W^{VI} [12], and Cd/Nb^V [13] cation couples exist in oxyfluorides. In these oxyfluorides, the evolution of the charge of M cations in the MO_xF_{6-x} octahedra is compensated by successive O/F substitutions. Oxygen atoms are found either at the axial bridging position between the central M^{II} cation and the M^V or M^{VI} cations (Cu/Nb^V, Cd/Nb^V) or at the equatorial positions (Cu/V^V), or both equatorial and non bridging axial positions (Cu/Mo^{VI}) or both equatorial and bridging axial positions (Cu/W^{VI}) of the MO_xF_{6-x} octahedra (Table 5). All trimer M^{II}–F–M^{IV} axes are parallel in fluorides while the trimer M^{II}–X–(M^V,M^{VI}) (X = O, F) axes lie in two perpendicular directions in oxyfluorides.

One other oxyfluoride with a reverse neutral trimer, $[H_3O]_2{\cdot}(Nb^VOF_5(CuF(py)_4)_2){\cdot}(F)_2$ [7], is isostructural with $[H_3O]_2{\cdot}(SiF_6(CuF(py)_4)_2){\cdot}(F)_2$ (**4**) (described in Section 3.2.2). Oxygen atoms are disordered with fluorine atoms on the axial bridging positions (Table 6).

3.3. Linear chains in $Cu(en)_2MF_6$ (5 and 6)

The structures of $Cu(en)_2MF_6$ (M^{IV} = Ti (**5**), Si (**6**)), involve neutral chains of alternating MF_6 and $(Cu(en)_2)F_2$ entities linked by opposite fluorine corners (Fig. 5). In **5** and **6**, the SiF_6 octahedra are regular while the TiF_6 octahedra are distorted with four short Ti–F(1) distances (1.746(5) Å) and two long Ti–F(2) distances (1.879(8) Å) (Table 7); as expected, the longest distances are associated with bridging fluorine atoms. The CuN_4F_2 octahedra are strongly distorted with short Cu–N distances and long Cu–F distances. The square planar coordination of copper by nitrogen

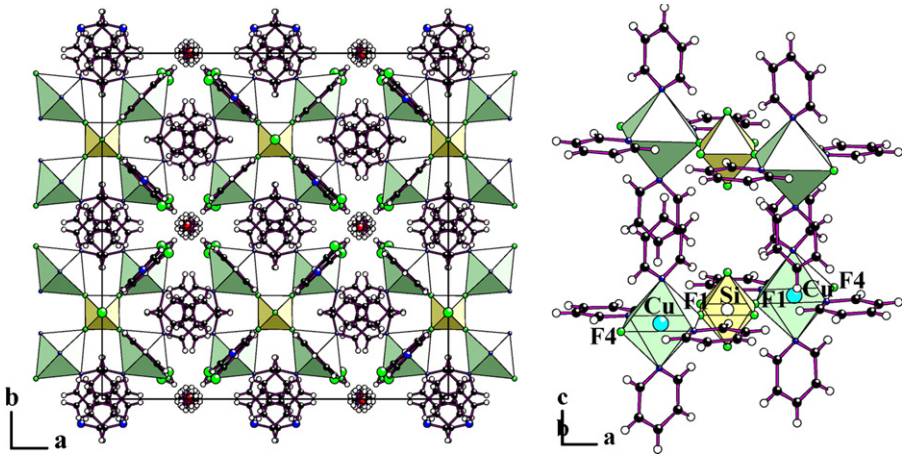

Fig. 3. [0 0 1] projection of the structure of $[H_3O]_2{\cdot}(SiF_6(CuF(py)_4)_2){\cdot}(F)_2$ (**4**) (left) and view of the neutral $SiF_6(CuF(py)_4)_2$ cluster (right).

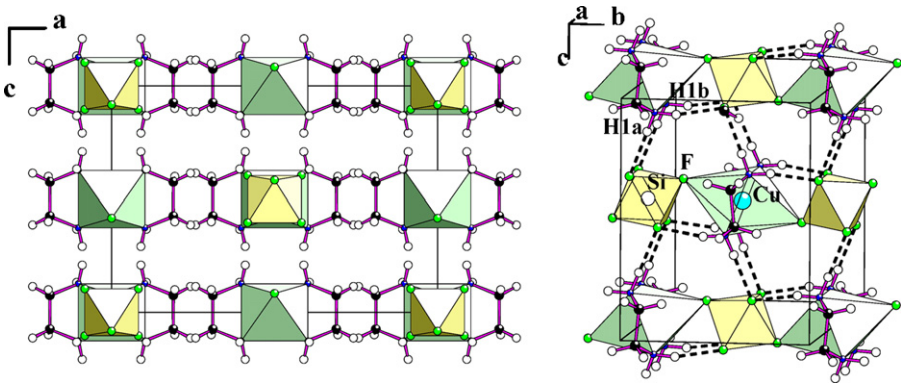

Fig. 5. [0 1 0] projection of $Cu(en)_2SiF_6$ (6) (left) and view of the $_\infty[Cu(en)_2SiF_6]$ chain (right).

Table 7
Selected inter-atomic distances (Å) and angles (°) in $(Cu(en)_2)\cdot(TiF_6)$ (**5**) and $(Cu(en)_2)\cdot(SiF_6)$ (**6**).

	CuTi (**5**)	CuSi (**6**)	Type[a]	Direction[a]
Cu–N	1.989(7) × 4	1.987(6) × 4		
Cu–F	2.430(8) × 2	2.580(4) × 2		
M^{IV}–F(1)	1.746(5) × 4	1.672(2) × 4		
M^{IV}–F(2)	1.879(8) × 2	1.676(2) × 2		
N(1)–H···F(1)	2.95(1)	2.851(5)	*intra*	*c*
N(1)–H···F(1)	2.80(1)	2.902(5)	*inter*	*b*
C(1)–H···F(1)	3.465(8)	3.320(5)	*inter*	*a*
Cu–F–M^{IV}	131.7(5)	131.6(3)		

[a] Type of hydrogen bonds (intrachain (*intra*) or interchain (*inter*)) and direction along which these bonds develop.

atoms is also distorted with two short N–N distances between nitrogen atoms of one distinct amine. The amines adopt a *cis* conformation and the dihedral N(1)–C(1)–C(1)–N(1) angle values are 15.9(2)° and 52.0(5)° for the titanium and silicon phases, respectively. Hydrogen bonds contribute to the stability of the structure with moderate N(1)–H(1a)···F(1) interchain interactions (Table 7 and Fig. 5 right) [14]. Intra-chain N(1)–H(1b)···F(1) hydrogen bonds imply a strong tilt of the octahedra from the *c* axis: the Cu–F–M^{IV} angles are 131.6(3)° in $Cu(en)_2SiF_6$ (**6**) and 131.7(5)° in $Cu(en)_2TiF_6$ (**5**). Such small angles are not found in other 1D mixed metal hybrid fluorides and, generally, the M–F–M angles do not deviate strongly from 180°. The smallest M–F–M values are found in two phases with the same previous cations and with pyrazine: 140.2(1)° in $Cu(pyz)(H_2O)_2TiF_6$ [15] and 141.2(1)° in $Cu(pyz)(H_2O)_2SiF_6$ [16]. Most of 1D fluorides exhibit linear *trans*-chains and no *cis*-chain is evidenced. However, a mixture of alternating *cis* and *trans* connections of SiF_6 and CuN_4F_2 octahedra exists in two phases, $(Cu(2\text{-}4'bpy)_4SiF_6)_2\cdot 4.5H_2O$ [17] and $(Cu(4\text{-}phpy)_4SiF_6)_2\cdot 4.5H_2O$ [17].

4. Conclusion

Six mixed M^{II}–M^{IV} hybrid fluorides crystallize in solvothermal conditions. They exhibit $M^{IV}F_6$, $M^{II}N_4F_2$ or $M^{II}N_6$ octahedral units in which nitrogen atoms come from neutral amines. The $M^{IV}F_6$ and $M^{II}N_6$ units are isolated in $(Ni(en)_3)\cdot(TiF_6)$. The $M^{IV}F_6$ and $M^{II}N_4F_2$ octahedra build trimetallic anionic $(Cu^{II}(py)_4(M^{IV}F_6)_2$, (M = Ti, Mo)) or neutral ($Si^{IV}F_6(Cu^{II}F(py)_4)_2$) clusters and infinite neutral chains ($Cu^{II}(en)_2M^{IV}F_6$ (M = Ti, Si)) by fluoride corner connection. When necessary, charge compensations are insured by H_3O^+ or protonated amines. In $[H_3O]_2\cdot(SiF_6(CuF(py)_4)_2)\cdot(F)_2$, it is shown that a position disorder affects the H_3O^+ cations and "free" F^- anions and, consequently the presence of H_2O and HF species cannot be excluded. In $[Hpy]_2\cdot(Cu(py)_4(MoF_6)_2)$, it is also shown that the oxidation state is +IV for molybdenum atoms and that O/F substitutions to give $(M^{(V)}OF_5)^{2-}$ or $(M^{(VI)}O_2F_4)^{2-}$ anions are probably excluded.

5. Experimental

All phases were synthesized from a mixture of the oxides (TiO_2 Riedel deHaën, MoO_2 Alfa Aesar, SiO_2, CuO or NiO Prolabo), hydrofluoric acid solution (48% HF, Prolabo), pyridine (*py*) (Prolabo), ethylenediamine (*en*) (Aldrich) and technical ethanol (EtOH). Details of the molar ratios $M^{IV}O_2/M^{II}O/py/en/HF/EtOH$ are given in Table 2. The solvothermal reaction was performed in a microwave oven (CEM Mars) using Teflon autoclaves. The heating program involved two steps after the addition of the reactants in the autoclave: dissolution of the metal oxides at 80 °C during 30 min, heating for 1 h at 160 °C. The solid products were washed with ethanol and dried at room temperature.

X-ray crystal data were collected at room temperature on a SIEMENS AED2 four-circle diffractometer (graphite monochromator Mo K_α) using $\omega/2\theta$ scans for **2** and **6** or an APEX II Quazar diffractometer (4-circle Kappa goniometer, IμS microfocus source, CCD detector) for **4**. The structure solutions were found by direct methods (TREF option) and extended by Fourier maps and subsequent refinements (SHELXS-86 and SHELXL-97 programs [18,19]). All non-hydrogen atoms were refined anisotropically whereas hydrogen atoms of amine were geometrically constrained (HFIX option). In the absence of single crystals, the structures of **1**, **3** and **5** were determined from X-ray powder data collected on a MPD-PRO diffractometer (PANalytical). Unit cells were obtained from the McMaille indexing software [20]. They were confirmed by a satisfying whole powder pattern fit (WPPF) by the Le Bail method [21] using the Fullprof software [22]. The extracted intensities were used for structure solution by direct space methods (ESPOIR software [23]). Then, Rietveld refinements were performed and good fits are obtained for the structures. Details of the structure determinations are given in Table 3. Rietveld patterns are presented in Supplementary Materials.

Acknowledgements

The authors are indebted to Dr. B. Boulard and Pr. C. Legein. Thanks are also due to the *Région des Pays de la Loire* for a doctoral grant (J. Lhoste, Perle project).

Appendix A. Supplementary data

Supplementary data associated with this article can be found, in the online version, at doi:10.1016/j.jfluchem.2011.03.021.

References

[1] C. Sanchez, F. Ribot, New J. Chem. 18 (1994) 1007–1047.
[2] K. Adil, M. Leblanc, V. Maisonneuve, P. Lightfoot, Dalton Trans. 39 (2010) 5983–5993.
[3] Q. Pan, J. Li, J. Yu, Y. Wang, Q. Fang, R. Xu, G. Xuexia, H. Xueba, Chem. J. Chin. Univ. 26 (2005) 2199–2200.
[4] Y. Li, Q. Shi, A.M.Z. Slawin, J.D. Woollins, J. Dong, Acta Crystallogr. E65 (2009) 1522.
[5] J. Hanikova, J. Kuchar, J. Cernak, G. Pelosi, Acta Crystallogr. E66 (2010) 1451–1452.
[6] T. Loiseau, F. Serpaggi, G. Férey, Z. Kristallography 219 (2004) 469–470.
[7] A.J. Norquist, M.E. Welk, C.L. Stern, K.R. Poeppelmeier, Chem. Mater. 12 (2000) 1905–1909.
[8] K.R. Heier, A.J. Norquist, C.G. Wilson, C.L. Stern, K.R. Poeppelmeier, Inorg. Chem. 37 (1998) 76–80.
[9] P. Halasyamani, M.J. Willis, C.L. Stern, P.M. Lundquist, G.K. Wong, K.R. Poeppelmeier, Inorg. Chem. 35 (1996) 1367–1371.
[10] M.E. Welk, A.J. Norquist, F.P. Arnold, C.L. Stern, K.R. Poeppelmeier, Inorg. Chem. 41 (2002) 5519–5525.
[11] M.E. Welk, A.J. Norquist, C.L. Stern, K.R. Poeppelmeier, Inorg. Chem. 39 (2000) 3946–3947.
[12] K.R. Heier, A.J. Norquist, P. Shiv Halasyamani, A. Duarte, C.L. Stern, K.R. Poeppelmeier, Inorg. Chem. 38 (1999) 762–767.
[13] P. Halasyamani, M.J. Willis, K.R. Heier, C.L. Stern, K.R. Poeppelmeier, Acta Crystallogr. C52 (1996) 2491–2493.
[14] T. Steiner, Angew. Chem. Int. Ed. 41 (2002) 48–76.
[15] P.A. Maggard, A.L. Kopf, C.L. Stern, K.R. Poeppelmeier, Cryst. Eng. Commun. 6 (2004) 451–457.
[16] K. Uemura, A. Maeda, T.K. Maji, P. Kanoo, H. Kita, Eur. J. Inorg. Chem. (2009) 2329–2337.
[17] C.H. Springsteen, R.D. Sweeder, R.L. LaDuca, Cryst. Growth Des. 6 (2006) 2308–2314.
[18] G.M. Sheldrick, SHELXS-86: A Program for Structure Solution, Göttingen University, Germany, 1986.
[19] G.M. Sheldrick, SHELXL-97: A Program for Crystal Structure Determination, Göttingen University, Germany, 1997.
[20] A. Le Bail, Powder Diffraction 19 (2004) 249–254.
[21] A. Le Bail, H. Duroy, J.L. Fourquet, Mat. Res. Bull. 23 (1988) 447–452.
[22] J. Rodriguez-Carvajal, J. Phys. B 192 (1993) 55–69.
[23] A. Le Bail, Mater. Sci. Forum. 378 (2001) 65–70.
[24] A.K. Cheetham, C.N.R. Rao, R.K. Feller, Chem. Commun. (2006) 4780–4795.
[25] M. Conner, A. McConnell, J. Schlueter, J. Manson, J. Low. Temp. Phys. 142 (2006) 273–278.
[26] M.-J. Lin, A. Jouaiti, N. Kyritsakas, M.W. Hosseini, Cryst. Eng. Commun. 12 (2010) 67–69.
[27] F.S. Keij, R.A.G. De Graaff, J.G. Haasnoot, J. Reedijk, E. Pedersen, Inorg. Chim. Acta 156 (1989) 65–70.
[28] R.A.J. Driessen, F.B. Hulsbergen, W.J. Vermin, J. Reedjik, Inorg. Chem. 21 (1982) 3595–3597.
[29] J.L. Manson, J.A. Schlueter, K.A. Funk, H.I. Southerland, B. Twamley, T. Lancaster, S.J. Blundell, P.J. Baker, F.L. Pratt, J. Singleton, R.D. McDonald, P.A. Goddard, P. Sengupta, C.D. Batista, L. Ding, C. Lee, M.-H. Whangbo, I. Franke, S. Cox, C. Baines, D. Trial, J. Am. Chem. Soc. 131 (2009) 6733–6747.
[30] M.-C. Suen, Z.-K. Chan, J.-D. Chen, J.-C. Wang, C.-H. Hung, Polyhedron 25 (2006) 2325–2332.
[31] M.-J. Lin, A. Jouaiti, D. Pocic, N. Kyritsakas, J.-M. Planeix, M.W. Hosseini, Chem. Commun. 46 (2010) 112–114.
[32] S.-I. Noro, R. Kitaura, M. Kondo, S. Kitagawa, T. Ishii, H. Matsuzaka, M. Yamashita, J. Am. Chem. Soc. 124 (2002) 2568–2583.
[33] S.-I. Noro, S. Kitagawa, M. Kondo, K. Seki, Angew. Chem. Int. Ed. 39 (2000) 2081–2084.
[34] S. Subramanian, M.J. Zaworotko, Angew. Chem. Int. Ed. 34 (1995) 2127–2129.
[35] M.-J. Lin, A. Jouaiti, N. Kyritsakas, M.W. Hosseini, Cryst. Eng. Commun. 11 (2009) 189–191.
[36] A.J. Norquist, K.R. Heier, C.L. Stern, K.R. Poeppelmeier, Inorg. Chem. 37 (1998) 6495–6501.
[37] M.-C. Suen, J.-C. Wang, Struct. Chem. 17 (2006) 315–322.
[38] T. Mahenthirarajah, Y. Li, P. Lightfoot, Inorg. Chem. 47 (2008) 9097–9102.